A semi-analytical model for predicting underwater noise radiated from offshore pile driving

Q. P. Deng, *W. K. Jiang

Institute of Vibration, Shock & Noise, Shanghai Jiao Tong University, China

*Corresponding author: wkjiang@sjtu.edu.cn

Abstract

It radiates high level of wideband underwater noise to drive large tubular piles into the seafloor by hydraulic impact hammers, which may detrimentally impact both fishes and marine mammals, such as dolphins and whales. Noise forecast and reduction is necessary in underwater engineering in order to protect the animals. In this study, a semi-analytical model is developed for predicting the vibration and the underwater sound radiation, where the pile is modeled as an elastic thin cylindrical shell. A modified variation methodology combined with the Reissner-Naghdi's thin shell theory is employed to formulate the mechanical model of the shell divided as several segments in axial direction. The sound pressures in both exterior and interior fluid fields are expressed as analytical series in frequency domain. The effect of the acoustic fluid on structural vibration is taken into consideration by incorporating the interface work done by the sound pressure into the total functional of the variation methodology. The underwater sound responses in both frequency domain and time domain are obtained from a case study. This mechanical model can be used to forecast underwater noise of piling and explore potential noise reduction measures to protect marine animals.

Keywords: Pile-driving, Cylindrical shell, Under-water noise, Structure-fluid interaction

Introduction

Offshore constructions increase quickly over the world, such as wind power generation platforms, petroleum and gas platforms, artificial islands and oversea bridges. These produce severe undersea noise pollution which has raised serious concerns from environmental protection organizations and academic world. Pile-driving noise is generally considered as the most severe underwater noise which would influence, harm or even kill marine animals inhabiting around piling sites, such as fishes, dolphins and whales (Madsen et al., 2006; Jefferson et al., 2009; Slabbekoorn et al., 2010). Research and prediction on the vibration and sound radiation of the pile is urgent and significant for the sake of ocean exploration and animal protection.

Some attempts have been in recent years made on the topic of underwater piling noise. The experimental results by Robinson et al. (2007) showed that the relationship between acoustic pulse energy and hammer energy had an approximate linear dependence during the soft start period of the piling procedure. Pile-driving underwater noise was detected at ranges of up to 70 km and behavioral disturbance may occur up to a distance of 50 km for bottlenose dolphins (Bailey et al., 2010). Underwater pressure field at approximate 10 m from the pile was found to be depth dependent in the tests of the authors (Stockham et al., 2010). Reinhall and Dahl (2010, 2011) studied the underwater piling noise by using a finite element model for the sound generation and parabolic equation model for propagation and found that the dominant underwater noise from impact driving is from the Mach wave associated with the radial expansion of the pile that propagates down the pile after impact at supersonic speed. A semi-analytical model for the prediction of underwater piling noise was established by Tsouvalas and Metrikine (2013), in which

the displacements of the shell was expanded over the in-vacuo vibration modes and the seabed soil was simplified to be distributed springs and dashpots. However, further investigation is required to develop a mechanical model with higher computational efficiency and accuracy.

In this study, a semi-analytical mechanical model is established for predicting the levels of underwater piling noise. A modified variation methodology is employed to formulate the mechanical model of the shell divided as several segments in axial direction. The sound pressures in both exterior and interior fluid fields are expressed as analytical functions. The effect of the acoustic fluid on structural vibration is considered by incorporating the interface work done by the sound pressure into the total functional of the variation statement. The radiated underwater noise in both frequency domain and time domain is illustrated based on a case study.

Basic Theory

Description of the model

The schematic diagram of the pile-driving model is illustrated in Figure 1. A pile is driving into the seabed by a hydraulic impact hammer. The pile is modeled as an elastic cylindrical shell with finite length and constant thickness. The hydraulic impact hammer is modeled as a force applied at the top of the pile. The seawater inside and outside the pile is assumed to be incompressible and inviscid. The effect of soil surrounding the pile is not taken into consideration and the pile is assumed to be fixed at the bottom. The sea surface Γ_2 is assumed to be a pressure released boundary, which means sound pressure vanishes on this surface. For the seabed Γ_3 two situations can be considered, i.e. a perfectly rigid boundary and a local impedance boundary. The constants $E, \mu, \eta, \rho_s, L, h$ and R correspond to the modulus of elasticity, Poisson ratio, structural loss factor, the density, length, thickness and radius of the mid-surface of the cylindrical shell, respectively. c, ρ_f are sound velocity and density of the seawater. The pile fills up interior fluid at $x_{is} < x < x_b$ and is surrounded by exterior fluid at $x_{es} < x < x_b$.

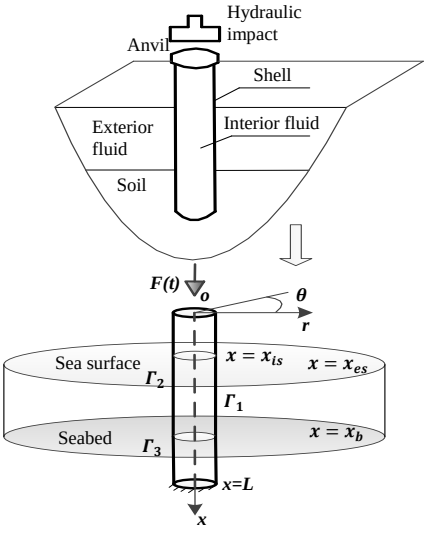

Figure 1. Pile-driving model

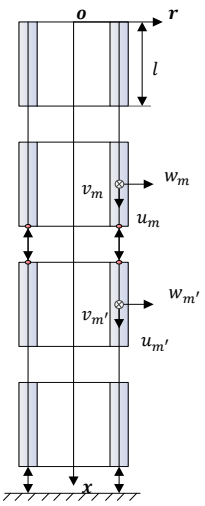

Figure 2. Structure decomposition

Structure decomposition model of pile

A modified variation methodology is used to establish the governing equations of the cylindrical shell. The methodology involves seeking the minimum of a modified functional as following equation (Qu, Chen et al., 2013).

$$\bar{\Pi}_{Tol} = \int_{t_0}^{t_1} \sum_{i=1}^{I} (T_i - U_i + W_i)\, dt + \int_{t_0}^{t_1} \sum_{i,i+1} \Pi_{\lambda\kappa}\ dt + \int_{t_0}^{t_1} \bar{\Pi}_{\lambda\kappa}\, dt \tag{1}$$

A variation form in the boundary value problem is generally mathematically easier than solving the common differential governing equations directly. The total energy functional of the mechanical system has extreme or stationary value only when the actual movement occurs. The extreme or stationary value of the energy functional can be obtained by expressing the solutions of the shell as the summation of a set of admissible displacement functions. In order to obtain reliable computational accuracy of high-frequency vibration, the shell is decomposed into *I* sub-shells with equal length l, as showed in Fig. 2. The requirement of interface continuity between two adjacent sub-shells can be satisfied by incorporating the continuity constraint conditions into the total energy functional by interface forces and least-squares weighted parameters. The geometrical boundaries at the bottom of the pile can also be satisfied by incorporated modified energy terms. The modifications on the total energy functional make the selection of admissible displacement functions flexible: the interface continuity conditions and geometrical boundary conditions will not be imposed on the displacement functions, but eventually satisfied in the variation statement.

The subscript i in equation (1) is the sub-shell number. T_i and U_i are kinetic energy and strain energy of the sub-shell, respectively. W_i is the work done by external force.

$$W_i = \iint_{S_i} (f_{u_i} u_i + f_{v_i} v_i + f_{w_i} w_i) R dx d\theta \tag{2}$$

$\Pi_{\lambda\kappa}$ is modified energy term incorporated from interface continuity conditions and geometrical boundary conditions at pile bottom, respectively. The incorporated modified term $\Pi_{\lambda\kappa}$ can be given as following form.

$$\begin{aligned} \Pi_{\lambda\kappa} = & \int_0^{2\pi} [N_x \Theta_u + \bar{N}_{x\theta} \Theta_v + \bar{Q}_x \Theta_w - M_x \Theta_r] R d\theta \\ & - \frac{1}{2} \int_0^{2\pi} [\kappa_u \Theta_u^2 + \kappa_v \Theta_v^2 + \kappa_w \Theta_w^2 - \kappa_r \Theta_r^2] R d\theta \end{aligned} \tag{3}$$

The function of the first integration term on the right side of equation (3) is to impose weak enforcement of kinematic interface continuity. $\Theta_u, \Theta_v, \Theta_v, \Theta_v$ are the essential continuity equations on the interface between adjacent sub-shells and are defined as $\Theta_u = u_i - u_{i+1}$, $\Theta_v = v_i - v_{i+1}$, $\Theta_w = w_i - w_{i+1}$,$\Theta_r = \partial w_i/\partial x - \partial w_{i+1}/\partial x$. $N_x, \bar{N}_{x\theta}, \bar{Q}_x, M_x$ are the resultant force in x direction, circumferential shear resultant force, lateral Kelvin-Kirchhoff shear resultant force and bending moment resultant force at the interface between two sub-shells, respectively. According to Reissner-Naghdi's shell theory, they can be written as equations (4)~(7).

$$N_x = K \left[\frac{\partial u_i}{\partial x} + \frac{\mu}{R} \left(\frac{\partial v_i}{\partial \theta} + w_i \right) \right] \tag{4}$$

$$\bar{N}_{x\theta} = \frac{1-\mu}{2} \left[K \left(\frac{1}{R} \frac{\partial u_i}{\partial \theta} + \frac{\partial v_i}{\partial x} \right) + \frac{D}{R^2} \left(\frac{\partial v_i}{\partial x} - 2 \frac{\partial^2 w_i}{\partial x \partial \theta} \right) \right] \tag{5}$$

$$\bar{Q}_x = D \left(\frac{1}{R^2} \frac{\partial^2 v_i}{\partial x \partial \theta} - \frac{\partial^3 w_i}{\partial x^3} - \frac{2-\mu}{R^2} \frac{\partial^3 w_i}{\partial x \partial \theta^2} \right) \tag{6}$$

$$M_x = D \left[-\frac{\partial^2 w_i}{\partial x^2} + \frac{\mu}{R^2} \left(\frac{\partial v_i}{\partial \theta} - \frac{\partial^2 w_i}{\partial \theta^2} \right) \right] \tag{7}$$

As shown in the second integrate term on the right side of equation (3), the least-squares weighted residual terms of the continuity equations are incorporated to further modify the total functional.

The functional of the least-squares weighted residual terms is to ensure a numerically stable operation for the structure decomposition methodology.

The incorporated modified term $\overline{\Pi}_{\lambda\kappa}$ in equation (1) is incorporated from geometrical boundary conditions at the bottom of the pile. $\overline{\Pi}_{\lambda\kappa}$ has the same form as $\Pi_{\lambda\kappa}$ and it can be obtained by substituting interface continuity equations by continuity equations of the geometry boundary, i.e. $\bar{\Theta}_u = u_I - \bar{u}$, $\bar{\Theta}_v = v_I - \bar{v}$, $\bar{\Theta}_w = w_I - \overline{w}$, and $\bar{\Theta}_r = \partial w_I/\partial x - \partial\overline{w}/\partial x$. u_I, v_I, w_I and $\partial w_I/\partial x$ are variables of the last sub-shell which is fixed at the bottom; $\bar{u}, \bar{v}, \overline{w}, \partial\overline{w}/\partial x$ are corresponding variables of the boundary and equal zero in this work.

Admissible displacement functions of shell

The displacement components u_i, v_i, w_i in $\overline{\Pi}_{\mathrm{Tol}}$ can be expanded in terms of admissible displacement functions and generalized coordinates. Due to the incorporation of the modified terms, the admissible displacement functions of each sub-shell are not constrained to satisfy any continuity conditions or geometrical boundary conditions. They are only required to be linearly independent, complete and differentiable. In this model, Fourier series for circumferential expansion and Chebyshev orthogonal polynomials for axial expansion are employed as the admissible displacement functions. The displacement components of each sub-shell can be written as following form.

$$u_i(x,\theta,t) = \sum_{m=1}^{M}\sum_{n=0}^{N}\sum_{\alpha=0}^{1} T_m(x)\cos\left(n\theta + \alpha\frac{\pi}{2}\right)\bar{u}_{mn\alpha}(t) = \boldsymbol{U}(x,\theta)\boldsymbol{u}_i(t) \tag{8}$$

$$v_i(x,\theta,t) = \sum_{m=1}^{M}\sum_{n=0}^{N}\sum_{\alpha=0}^{1} T_m(x)\sin\left(n\theta + \alpha\frac{\pi}{2}\right)\bar{v}_{mn\alpha}(t) = \boldsymbol{V}(x,\theta)\boldsymbol{v}_i(t) \tag{9}$$

$$w_i(x,\theta,t) = \sum_{m=1}^{M}\sum_{n=0}^{N}\sum_{\alpha=0}^{1} T_m(x)\cos\left(n\theta + \alpha\frac{\pi}{2}\right)\overline{w}_{mn\alpha}(t) = \boldsymbol{W}(x,\theta)\boldsymbol{w}_i(t) \tag{10}$$

where $T_m(x)$ is the m order Chebyshev polynomials. M, N are the highest degrees taken in the polynomials and series, respectively. $\boldsymbol{U}(x,\theta), \boldsymbol{V}(x,\theta), \boldsymbol{W}(x,\theta)$ are admissible displacement function vectors of the three directions. $\boldsymbol{u}_i(t), \boldsymbol{v}_i(t), \boldsymbol{w}_i(t)$ are corresponding generalized coordinate vectors.

Pressure in fluid domain

Under some regular boundary conditions, fluid pressure in frequency domain can be expanded as a summation of analytical functions by applying variable separation technique in a circular cylindrical coordinates. The analytical expression of the fluid pressure allows one to examine qualitatively the influence of a number of parameters on the underwater sound radiation. For the fluid domain outside the pile, the fluid pressure and the velocity component normal to the surface of the shell can be given as equation (11) and (12) (Tsouvalas and Metrikine, 2013).

$$\tilde{p}_e(x,r,\theta) = -i\omega\rho_f \sum_{\alpha=0}^{1}\sum_{n=0}^{\infty}\sum_{p=0}^{\infty} D_{np}H_n^{(2)}(k_{rp}r)\sin k_{xp}(x - x_{es})\cos(n\theta + \alpha\frac{\pi}{2}) \tag{11}$$

$$\tilde{v}_{er}(x,r,\theta) = \sum_{\alpha=0}^{1}\sum_{n=0}^{\infty}\sum_{p=0}^{\infty} D_{np}H_n^{\prime(2)}(k_{rp}r)\sin k_{xp}(x - x_{es})\cos(n\theta + \alpha\frac{\pi}{2}) \tag{12}$$

where ρ_f is the density of the fluid. $H_n^{(2)}$ is the Hankel function of the second kind and of order n. $H_n'^{(2)}$ denotes its derivative with respect to r. k_{xp}, k_{rp} are wave number in x direction and r direction respectively and they are determined by radian frequency ω and boundary conditions at sea surface and seabed. D_{np} are unknown coefficients which can be determined by normal displacement on structure-fluid coupling interface Γ_1.

Assume there are I_e sub-shells submerged fully or partly in the exterior fluid. the i-th submerged sub-shell stretches over the axial coordinate interval $[x_i,\ x_{i+1}]$, and the coupling area on i-th submerged sub-shell occupies coordinate interval $[\bar{x}_i,\ \bar{x}_{i+1}]$. For fully submerged shell, $[x_i,\ x_{i+1}]$ is expressed by $[\bar{x}_i,\ \bar{x}_{i+1}]$. Based on the normal displacement given in equation (10), the normal displacement on the entire shell-fluid coupling interface can be written as

$$w_r(x,\theta,t) = \sum_{i=1}^{I_e} w_{ri}(x,\theta,t) * [H(x-\bar{x}_i) - H(x-\bar{x}_{i+1})], \quad (x_{es} < x < x_b)$$
$$\text{With:} \quad w_{ri}(x,\theta,t) = \textstyle\sum_{m,n,\alpha} w_{imn\alpha}\, T_m(x-x_i)\, cos\left(n\theta + \alpha\frac{\pi}{2}\right) e^{i\omega t} \tag{13}$$

$H(x-\bar{x}_i)$ is the Heaviside step function. On the coupling interface, the normal velocity continuity condition should be satisfied. Combining equations (12) and (13), the normal velocity continuity equations is given as

$$i\omega \sum_{i=1}^{I_e} \sum_{m,n,\alpha} w_{imn\alpha}\, T_m(x-x_i)\, cos\left(n\theta + \alpha\frac{\pi}{2}\right) [H(x-\bar{x}_i) - H(x-\bar{x}_{i+1})]$$
$$= \sum_{\alpha=0}^{1} \sum_{n=0}^{\infty} \sum_{p=0}^{\infty} D_{np} H_n'^{(2)}(k_{rp} r) \sin k_{xp}(x-x_{es}) \cos(n\theta + \alpha\frac{\pi}{2}) \tag{14}$$

By making use of orthogonality property of fluid modes, the unknown coefficient D_{np} can be obtained. Then the pressure in the exterior fluid domain can be expressed by analytical functions weighted by generalized coordinates of normal displacements, as shown in equation (15).

$$\tilde{p}_e(x,r,\theta,\omega) = \sum_{\alpha=0}^{1} \sum_{n=0}^{\infty} \sum_{i=0}^{I_e} \sum_{p=0}^{\infty} \sum_{m=1}^{M} w_{imn\alpha} \cdot \tilde{P}_{e,inmp\alpha} \quad \text{with:}$$

$$\tilde{P}_{e,inmp\alpha} = \frac{\omega^2 \rho}{f_p} \frac{H_n^{(2)}(k_{rp} r)}{H_n'^{(2)}(k_{rp} R)} \cdot \sin k_{xp}(x-x_{es}) \cdot \cos(n\theta + \alpha\frac{\pi}{2}) \tag{15}$$
$$\cdot \int_{\bar{x}_i}^{\bar{x}_{i+1}} T_m(x-x_i) \cdot \sin k_{xp}(x-x_{es})\, dx$$

The derivation procedure of fluid pressure inside the pile is completely analogous as that of interior fluid pressure.

Governing equations of shell-fluid coupling vibration

Interaction between the pile wall and contiguous fluid has a profound influence on the magnitude and phase of the structural vibration. Use 'fluid loading' to describe the effect that the fluid has on the shell vibration (Fahy and Gardonio, 2007). The fluid pressure given in (15) is regarded as fluid loading acting on the pile wall. The work done by the exterior fluid pressure on the coupling interface is given as following equation

$$W_p = \int_0^{2\pi} \int_{x_s}^{x_b} -pw_r R dx\, d\theta \tag{16}$$

Fourier transform pairs with respect to time are introduced herein to transform variables between time domain and frequency domain. By substituting the work done by fluid pressure and the work done by hydraulic impact force into the total functional $\overline{\Pi}_{Tol}$ and performing the variation operation with respect to the generalized coordinate vectors $\boldsymbol{u}$, $\boldsymbol{v}$, and $\boldsymbol{w}$, the governing equations of motion of the pile can be obtained as

$$[-\omega^2 \boldsymbol{M} + (\boldsymbol{K} - \overline{\boldsymbol{K}}_{\boldsymbol{\lambda}} + \overline{\boldsymbol{K}}_{\boldsymbol{\kappa}}) - \boldsymbol{C}_{\boldsymbol{e}} + \boldsymbol{C}_{\boldsymbol{i}}]\boldsymbol{q}(\omega) = \boldsymbol{F}(\omega) \tag{17}$$

where $\boldsymbol{M}$ and $\boldsymbol{K}$ are mass matrix and stiffness matrix, respectively. $\overline{\boldsymbol{K}}_{\boldsymbol{\lambda}}$ and $\overline{\boldsymbol{K}}_{\boldsymbol{\kappa}}$ are the generalized interface stiffness matrixes introduced by the interface forces and the least-squares weighted residual parameters, respectively. $\boldsymbol{C}_{\boldsymbol{e}}$ and $\boldsymbol{C}_{\boldsymbol{i}}$ are coupling matrixes introduced by fluid pressure in exterior fluid domain and interior fluid domain. $\boldsymbol{q}(\omega) = [\boldsymbol{u}_1^T, \boldsymbol{v}_1^T, \boldsymbol{w}_1^T, \boldsymbol{u}_2^T, \boldsymbol{v}_2^T, \boldsymbol{w}_2^T, \cdots, \boldsymbol{u}_I^T, \boldsymbol{v}_I^T, \boldsymbol{w}_I^T]$ is the global generalized coordinate vector of the shell and $\boldsymbol{F}(\omega)$ is the generalized force vector. Responses in time domain can be obtained by performing Fourier inverse transformation to frequency responses.

Computational results and discussion

A pile with a certain geometry and material parameters is chosen for numerical case. The seabed is assumed to be perfectly rigid acoustic boundary. The hydraulic impact force is assumed to be an averagely distributed line force $F(t)$, which is parallel with x axis, acting on the intersecting line of the middle surface of the shell and cross section on the pile top. The material properties of the shell, geometry and parameters of the model are summarized in Table 1.

Table 1. Model parameters

Part	Parameters
Shell	Geometry: $L = 16m, R = 2.2m, h = 50mm$ Material parameters: $E = 2.1 \times 10^{11}, \rho_s = 7800kg\ m^{-3}, \mu = 0.3, \eta = 0.005$ Decomposition parameters: *M=8, I=7, N=0*
Fluid	$c = 1400m\ s^{-1}, \rho_f = 1000kg\ m^{-3},\ x_{es} = 4, x_{is} = 4, x_b = 12$
Force	$F(t) = \begin{cases} 1 \times 10^5 N/m & (0 < t < 1\ ms) \\ 0 & (t \le 0\ or\ t \ge 1\ ms) \end{cases}$

Fig. 3 shows the frequency spectrum and time history of sound pressure at observing position A which is located 4 meters under the sea surface and 8 meters away from the pile surface. As can be seen from the Figure, frequency spectrum of SPL at position A has 2 dominant peaks at 80 Hz and 140 Hz, respectively. The SPL curve has a remarkable nadir at around 1000 Hz. The history of sound pressure at position A sees its first peak at about 7 ms, which means it takes about 7 ms from the very beginning moment when the hydraulic impact acts on the pile top to the moment when the peak of the first pressure wave arrives at the position. Then the pressure decreases stablely over the time axis, albeit with slight fluctuations.

Fig. 4 shows SPL distributions on the $x - r$ plane at $\theta = 0\ rad$ for three different frequencies, i.e. 100 Hz, 200 Hz and 800 Hz. The pressure fields see an obvious attenuation trend as the radial distance increases and form distinct standing waves along the vertical axis. The sea surface plane and the seabed plane form an acoustic waveguide. Sound reflection in the acoustic waveguide produces standing waves in vertical direction. The existence of standing waves in vertical direction demonstrates that the fluid pressure is depth dependent.

From Fig. 4 the wavelength of the standing wave decreases as the frequency ascends. The dominant modes of high-frequency vibration have relatively small wavelengths in vertical direction for axisymmetric vibration. Therefore high-frequency sound has relatively small wavelengths in vertical direction due to the requirement of normal velocity continuity conditions.

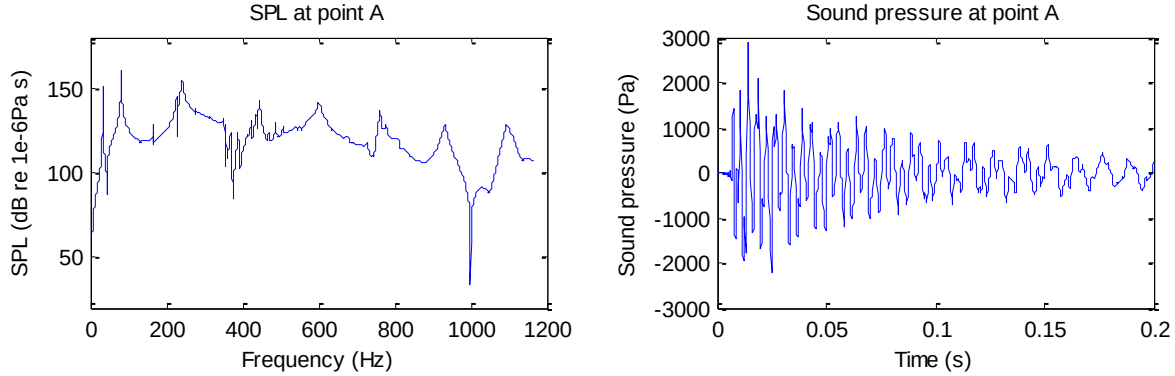

(a) Frequency spectrum **(b) Time history of sound pressure**

Figure 3. Sound at point A

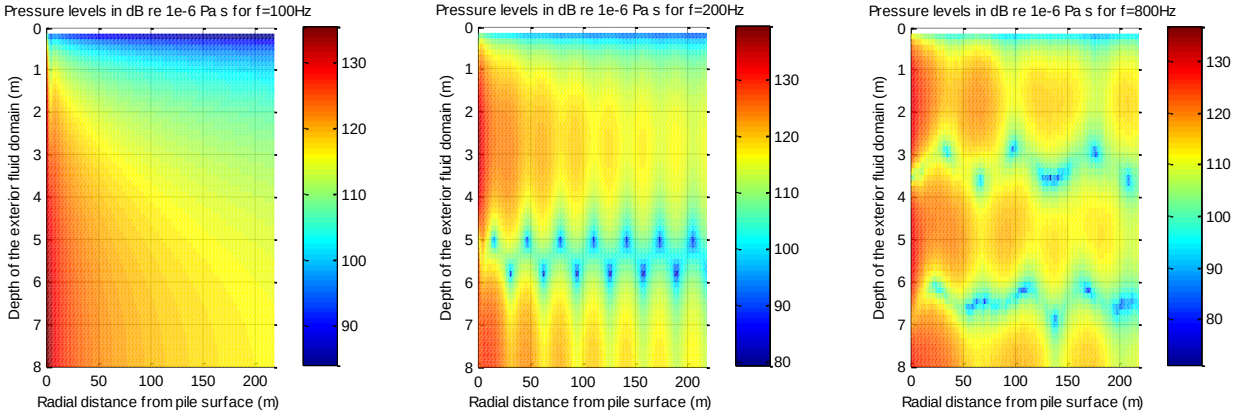

(a) f=100 Hz **(b) f=200 Hz** **(c) f=800 Hz**

Figure 4. Distributions of sound pressure in the section plane

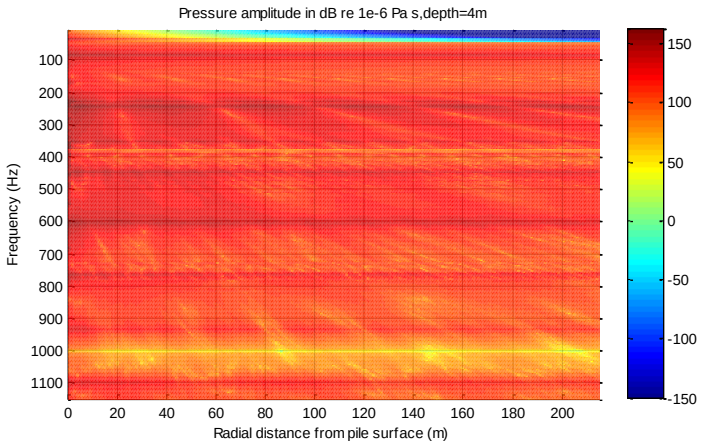

Figure 5. Sound pressure level vs. radial distance

Fig. 5 shows the attenuation of the pressure levels 4 meters under the sea surface for frequencies ranging from 5 Hz to 1150 Hz and for radial distances up to 215 m from the pile surface. It's obviously indicated at the top of the figure that no pressure waves can effectively propagate away

from the pile in the exterior fluid for frequencies lower than the cut-off frequency (about 42 Hz), which demonstrates the exterior fluid domain has a filtering function for relatively low frequencies. For perfectly rigid seabed, radial wavenumber can be expressed as $k_{rp} = \sqrt{\left(\frac{\omega}{c}\right)^2 - \left[\frac{2p+1}{2(x_b - x_{es})}\right]^2}$. The radiation condition at $r \to \infty$ requires that $Re(k_{rp}) \geq 0$ and $Im(k_{rp}) \leq 0$. According to equation (15), when $Im(k_{rp}) < 0$, $\tilde{P}_{e,inmp\alpha}$ will decrease along r axis nearly in the form of exponential attenuation. Hence the cut-off frequency can be given as $f_c = \frac{c}{2\pi} \cdot \frac{2p_{min}+1}{2(x_b - x_{es})}$. It is obvious that the cut-off frequency f_c is inversely proportional to the depth of the exterior fluid field.

As shown in Fig.5, sound pressures on frequencies around 80 Hz, 240 Hz, 450 Hz, 600 Hz and 760 Hz are dominant at this depth, while pressure level of 1000 Hz is much lower than pressure levels of other frequencies.

Conclusions

A computationally efficient semi-analytical mechanical model has been established for predicting underwater noise radiated from offshore pile driving, in which the coupling effect between pile and fluid is taken into consideration. A modified variation methodology is employed to formulate the mechanical model and the shell is divided as several segments in axial direction. The methodology creates considerable flexibility in the selection of admissible displacement functions and significantly simplifies the solving progress of the coupling vibration. A case study shows that the pressure amplitude at the observing position declines steadily during the duration after the first pressure wave arrives, albeit with slight fluctuations. The fluid pressure in frequency domain form standing waves in vertical direction and the wavelengths of the standing waves descend as the frequency increases, which indicates that the underwater sound pressures are depth dependent. A cut-off frequency for sound propagating is found in the exterior fluid domain and it is inversely proportional to the depth of the exterior fluid field. No sound can propagate effectively away from the pile for frequencies lower than the cut-off frequency.

References

Madsen, P. T., Wahlberg, M., Tougaard, J., Lucke, K. and Tyack, P. (2006), Wind turbine underwater noise and marine mammals: implications of current knowledge and data needs. *Marine Ecology-Progress Series*, 309, pp. 279-295.

Jefferson, T. A., Hung, S. K. and Wursig, B. (2009), Protecting small cetaceans from coastal development: Impact assessment and mitigation experience in Hong Kong. *Marine Policy*, 33(2), pp. 305-311.

Slabbekoorn, H., Bouton, N., van Opzeeland, I., Coers, A., ten Cate, C. and Popper, A. N. (2010), A noisy spring: The impact of globally rising underwater sound levels on fish. *Trends in Ecology and Evolution*, 25(7), pp. 419-427.

Robinson, S. P., Lepper, P. A. and Ablitt, J. (2007), The measurement of the underwater radiated noise from marine piling including characterisation of a "soft start" period. *OCEANS 2007-Europe*.

Bailey, H., Senior, B., Simmons, D., Rusin, J., Picken, G. and Thompson, P. M. (2010), Assessing underwater noise levels during pile-driving at an offshore windfarm and its potential effects on marine mammals. *Marine Pollution Bulletin*, 60(6), pp. 888-897.

Stockham, M. L., Dahl, P. H. and Reinhall, P. G. (2010), Characterizing underwater noise from industrial pile driving at close range. *2010 Oceans Mts/Ieee Seattle*.

Reinhall, P. G. and Dahl, P. H. (2010), Acoustic radiation from a submerged pile during pile driving. *2010 Oceans Mts/Ieee Seattle*.

Reinhall, P. G. and Dahl, P. H. (2011), Underwater Mach wave radiation from impact pile driving: Theory and observation. *Journal of the Acoustical Society of America*, 130(3), pp. 1209-1216.

Tsouvalas, A. and Metrikine, A. V. (2013), A semi-analytical model for the prediction of underwater noise from offshore pile driving. *Journal of Sound and Vibration*, 332(13), pp. 3232-3257.

Qu, Y. G., Chen, Y., Long, X. H., Hua, H. X. and Meng, G. (2013), Free and forced vibration analysis of uniform and stepped circular cylindrical shells using a domain decomposition method. *Applied Acoustics*, 74(3), pp. 425-439.

Fahy, F. J. and Gardonio, P. (2007). Sound and Structural Vibratin: Radiation, Transmission and Response, *Elsevier Science*.